Thermoelectric corrections to quantum voltage measurement

Justin P. Bergfield*
Department of Chemistry, Northwestern University, Evanston, Illinois, 60208, USA

Charles A. Stafford
Department of Physics, University of Arizona, 1118 East Fourth Street, Tucson, Arizona 85721, USA

(Received 8 September 2014; revised manuscript received 27 October 2014; published 29 December 2014)

A generalization of Büttiker's voltage probe concept for nonzero temperatures is an open third terminal of a quantum thermoelectric circuit. An explicit analytic expression for the thermoelectric correction to an ideal quantum voltage measurement in linear response is derived and interpreted in terms of local Peltier cooling/heating within the nonequilibrium system. The thermoelectric correction is found to be large (up to ±24% of the peak voltage) in a prototypical ballistic quantum conductor (graphene nanoribbon). The effects of measurement nonideality are also investigated. Our findings have important implications for precision local electrical measurements.

DOI: 10.1103/PhysRevB.90.235438 PACS number(s): 07.79.Cz, 72.15.Jf, 72.80.Vp, 84.37.+q

I. INTRODUCTION

Following the work of Engquist and Anderson [1], Büttiker developed a paradigm [2–4] of quantum voltage measurement carried out by a probe consisting of a reservoir of noninteracting electrons coupled locally to a system of interest. The probe exchanges electrons with the system until it reaches local electrical equilibrium with the system:

$$I_p^{(0)} = 0, \tag{1}$$

where $-eI_p^{(0)}$ is the mean electrical current flowing into the probe. Once equilibrium is established, the chemical potential $\mu_p \equiv -eV_p$ of the probe constitutes a measurement of the local electrochemical potential (and voltage V_p) within the nonequilibrium quantum system [3]. Condition (1) implies the probe has a large electrical input impedance, a necessary condition for a faithful voltage measurement. Scanning potentiometers satisfying these conditions [5] are now a mature technology, and many experiments in mesoscopic electrical transport utilize voltage probes as circuit components [6–9].

Although the average electric current into the probe is zero, electrons are constantly being emitted from the system into the probe and are replaced by electrons from the probe reservoir whose quantum-mechanical phase is uncorrelated with those emitted by the system. In this way, such a voltage probe serves as an *inelastic scatterer* [2], analogous to the model of inelastic scattering introduced previously in the context of lattice thermal conduction [10,11]. Indeed, much of the theoretical interest in Büttiker's model of a voltage probe is as a convenient way to introduce inelastic scattering in a quantum-coherent conductor at the expense of introducing one additional electrical terminal.

Büttiker's early analysis [2,3] was confined to systems at absolute zero temperature, where thermoelectric effects are absent. More recently, voltage probes at finite temperature have been considered by a number of investigators in various contexts and limits [4,12–16]. In particular, Förster *et al.* [4] considered the limit where the thermal coupling of the probe to the environment is large, so that the probe remains at ambient temperature despite its coupling to the nonequilibrium quantum system [4]. This limit is consistent with the original analysis of Engquist and Anderson [1], which did not consider thermoelectric effects.

However, considered as a model of an inelastic scatterer, a voltage probe cannot be a steady-state source or sink of heat [13]. This suggests that in generalizing the voltage probe concept [2,3] to finite temperatures, the probe should be not only in local electrical equilibrium but also in local thermal equilibrium with the system:

$$I_p^{(1)} = 0, \tag{2}$$

where $I_p^{(1)}$ is the heat current flowing into the probe. Condition (2) is required for a probe with a large thermal input impedance.

Further support for the additional condition (2) is provided by considering thermoelectric effects in the three-terminal circuit formed by the system with source, drain, and probe. Even if both source and drain electrodes are held at ambient temperature, an electrical bias between source and drain can drive Peltier cooling/heating within the system, resulting in hot and cold spots that differ significantly from ambient temperature. If the probe is not allowed to equilibrate thermally with the system under these conditions, a voltage will develop across the system-probe junction due to the Seebeck effect. Then the probe voltage can no longer be interpreted as a measurement of the local electrochemical potential in the system. We thus define an *ideal voltage measurement* as one satisfying both conditions (1) and (2). A precision voltage measurement thus requires a simultaneous precision temperature measurement.

A significant challenge to achieving such an ideal voltage measurement is posed by thermal coupling of the probe to the environment [17–20], including to the system's lattice [4], which may not be in local thermal equilibrium with the nonequilibrium electron system. Furthermore, this coupling may be many times larger than the probe's local thermal coupling to the system's electrons [18–20]. The probe's thermal coupling to anything other than the nonequilibrium electron system of interest leads to a deviation of the

*justin.bergfield@northwestern.edu

probe's voltage from the ideal value associated with the local electrochemical potential of the system and thus must be considered a nonideality. The probe's thermal coupling to the system's lattice can be minimized when it is operated in the tunneling regime [19], and continued advances in scanning thermal microscopy (SThM) [17,18,21–23] promise to further reduce the probe's thermal coupling to the environment.

II. LINEAR THERMOELECTRIC RESPONSE

In the limit of small electric and thermal bias away from the equilibrium temperature T_0 and chemical potential μ_0, the electric current $-eI_p^{(0)}$ and heat current $I_p^{(1)}$ flowing into the probe may be expressed as [19,24]

$$\begin{aligned} I_p^{(\nu)} =& \mathcal{L}_{p1}^{(\nu)}(\mu_1-\mu_p)+\mathcal{L}_{p2}^{(\nu)}(\mu_2-\mu_p) \\ &+ \mathcal{L}_{p1}^{(\nu+1)}\left(\frac{T_1-T_p}{T_0}\right)+\mathcal{L}_{p2}^{(\nu+1)}\left(\frac{T_2-T_p}{T_0}\right) \\ &+ \delta_{\nu,1}\kappa_{p0}(T_0-T_p), \end{aligned} \tag{3}$$

where $\mathcal{L}_{\alpha\beta}^{(\nu)}$ are Onsager linear-response coefficients with electrode labels α and β and $\kappa_{p0}=\mathcal{L}_{p0}^{(2)}/T_0$ is the thermal conductance between the probe and the ambient environment [19]. Equation (3) is a *completely general* linear-response formula and applies to macroscopic systems, mesoscopic systems, nanostructures, etc., including electrons, phonons, and all other degrees of freedom, with arbitrary interactions between them.

At sufficiently low temperatures or for sufficiently small systems, the electronic contribution to the coefficients $\mathcal{L}_{\alpha\beta}^{(\nu)}$ may be calculated using elastic quantum transport theory [25–27]

$$\mathcal{L}_{\alpha\beta}^{(\nu)}=\frac{1}{h}\int dE\,(E-\mu_0)^{\nu}\,T_{\alpha\beta}(E)\left(-\frac{\partial f_0}{\partial E}\right), \tag{4}$$

where $T_{\alpha\beta}(E)$ is the quantum-mechanical transmission function [28] describing the probability to propagate from electrode β to electrode α, and

$$f_0(E)=\frac{1}{\exp\left(\frac{E-\mu_0}{k_BT_0}\right)+1} \tag{5}$$

is the equilibrium Fermi-Dirac distribution.

A. Büttiker's voltage probe

In the limit as the system temperature approaches absolute zero, Eq. (4) becomes

$$\lim_{T_0\to 0}\mathcal{L}_{\alpha\beta}^{(\nu)}=\frac{1}{h}T_{\alpha\beta}(\mu_0)\delta_{\nu,0}. \tag{6}$$

Then Eqs. (1) and (3) may be solved to obtain Büttiker's result [2,3] for the voltage measured by the probe,

$$\mu_p^{\mathrm{B}}\equiv\lim_{T_0\to 0}\mu_p=\frac{T_{p1}(\mu_0)\mu_1+T_{p2}(\mu_0)\mu_2}{T_{p1}(\mu_0)+T_{p2}(\mu_0)}. \tag{7}$$

B. Engquist and Anderson's voltage probe

The question of how to generalize Büttiker's result (7) to systems at nonzero temperatures remains. Early on, Engquist and Anderson [1] considered both voltage and temperature probes of quantum electron systems at finite temperature. For the case of a voltage measurement, they assumed the entire system remains at ambient temperature $T_1=T_2=T_p=T_0$, so that Eqs. (1) and (3) imply

$$\mu_p^{\mathrm{EA}}=\frac{\mathcal{L}_{p1}^{(0)}\mu_1+\mathcal{L}_{p2}^{(0)}\mu_2}{\mathcal{L}_{p1}^{(0)}+\mathcal{L}_{p2}^{(0)}}. \tag{8}$$

However, substituting Eq. (8) for the probe's chemical potential into Eq. (3) gives

$$I_p^{(1)}=\frac{\mathcal{L}_{p1}^{(1)}\mathcal{L}_{p2}^{(0)}-\mathcal{L}_{p2}^{(1)}\mathcal{L}_{p1}^{(0)}}{\mathcal{L}_{p1}^{(0)}+\mathcal{L}_{p2}^{(0)}}(\mu_1-\mu_2), \tag{9}$$

which is generally nonzero at finite temperature. This is a generic three-terminal thermoelectric effect occurring whenever the probe coupling to the source and drain electrodes (through the system) is unequal. Thus the voltage probe originally proposed by Engquist and Anderson is *not in thermal equilibrium* with the system. In the absence of thermal equilibrium, the identification of μ_p^{EA} with the local electrochemical potential of the system is problematic since any temperature differential between sample and probe will lead to a voltage differential through the Seebeck effect. Moreover, the assumption that $T_p=T_0$ is inconsistent, given that $I_p^{(1)}\neq 0$, unless the thermal coupling of the probe to the environment is so large that the heat current flowing into the probe from the system can be neglected.

III. IDEAL VOLTAGE MEASUREMENT

We define an ideal voltage measurement as one in which the probe is in *both electrical equilibrium and thermal equilibrium* with the system. For an electrical bias $\Delta\mu=\mu_1-\mu_2$ applied between electrodes 1 and 2, both held at ambient temperature ($T_1=T_2=T_0$), Eqs. (1)–(3) can be solved for the probe voltage of such an ideal measurement, yielding $\mu_p=\mu_p^{\mathrm{EA}}-e\Delta V_p$, where the thermoelectric correction to the voltage is

$$\Delta V_p=S_{ps}(T_p-T_0), \tag{10}$$

$$S_{ps}=-\frac{1}{eT_0}\frac{\mathcal{L}_{p1}^{(1)}+\mathcal{L}_{p2}^{(1)}}{\mathcal{L}_{p1}^{(0)}+\mathcal{L}_{p2}^{(0)}} \tag{11}$$

is the thermopower of the probe-sample junction, and T_p is the probe temperature satisfying

$$T_p-T_0=\frac{I_p^{(1)}}{\kappa_{ps}+\kappa_{p0}}, \tag{12}$$

where $I_p^{(1)}$ is given by Eq. (9),

$$\kappa_{ps}=\frac{1}{T_0}\left[\left(\mathcal{L}_{p1}^{(2)}+\mathcal{L}_{p2}^{(2)}\right)-\frac{\left(\mathcal{L}_{p1}^{(1)}+\mathcal{L}_{p2}^{(1)}\right)^2}{\left(\mathcal{L}_{p1}^{(0)}+\mathcal{L}_{p2}^{(0)}\right)}\right] \tag{13}$$

is the parallel thermal conductance from electrodes 1 and 2 into the probe, and κ_{p0} is the thermal coupling of the probe to the environment at temperature T_0.

IV. RESULTS

In this section, we calculate the thermoelectric correction to the probe voltage for a prototypical ballistic quantum conductor, a graphene nanoribbon. However, we emphasize that the voltage error induced by thermoelectric effects is a generic phenomenon and not material specific. Figure 1 shows the computed voltage distribution for a zigzag graphene nanoribbon with an electrical bias of 0.1 V between the source and drain electrodes (at the right and left in the figure), which are held at the ambient temperature of $T_0 = 300$ K. The equilibrium chemical potential of the nanoribbon (determined by doping and/or a back gate) was taken to be $\mu_0 - \mu_{\rm Dirac} = -57.5$ meV. In the top panel of Fig. 1, an oscillatory pattern can be observed, superimposed on the overall voltage drop between the two electrodes. This is a manifestation of the characteristic voltage oscillations predicted by Büttiker [3], arising in this case from the interference of electron waves propagating directly from an electrode into the probe and waves scattered from the edges of the nanoribbon.

In our calculations, the π system of the graphene nanoribbon is described using a tight-binding model which has been shown to accurately reproduce the low-energy physics of this system [29]. The macroscopic electrodes are assumed to operate in the broadband limit, where the electrode-nanoribbon coupling is independent of energy, with a per-orbital bonding strength of 2.5 eV. The voltage probe is modeled as an atomically sharp Pt tip scanned at a fixed height of 3 Å above the plane of the C nuclei (tunneling regime). The tunneling matrix elements between the probe atoms and the nanoribbon

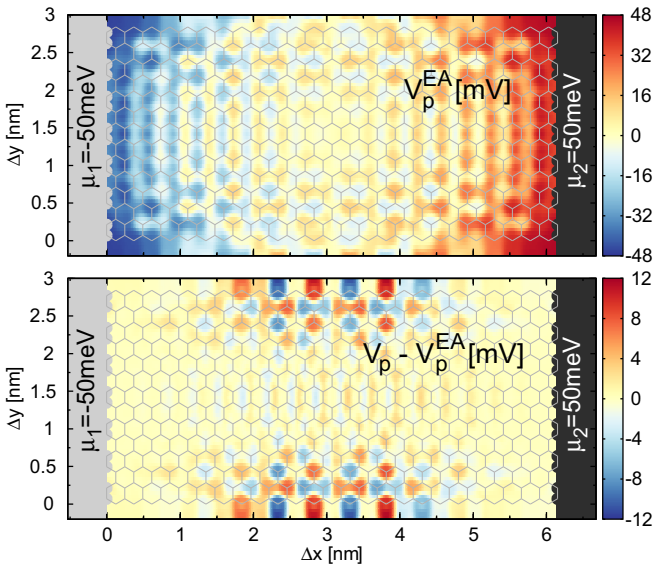

FIG. 1. (Color online) The calculated response of a voltage probe scanned 3 Å above the plane of a zigzag graphene nanoribbon. (top) The voltage distribution calculated using Engquist and Anderson's theory [1] [see Eq. (8)]. This theory neglects thermoelectric effects. The peak voltage for this system is 47.6 mV. (bottom) The thermoelectric correction ΔV_p to the probe voltage, calculated using Eqs. (10)–(13), reaching a maximum value for this system of 11.5 mV. Calculations are performed at $\mu_0 - \mu_{\rm Dirac} = -57.5$ meV, $\mu_2 - \mu_1 = 0.1$ eV, $T_1 = T_2 = T_0 = 300$ K, and $\kappa_{p0} = 0$.

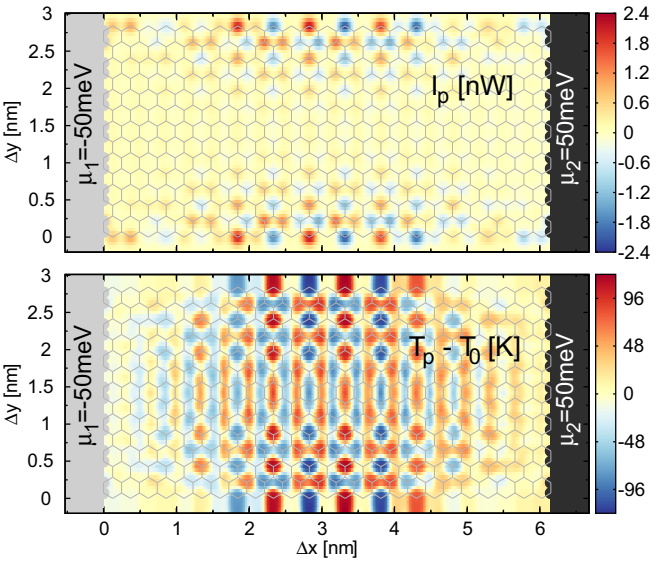

FIG. 2. (Color online) (top) The heat current $I_p^{(1)}$ flowing into the probe when it is held at the ambient temperature $T_0 = 300$ K, calculated from Eq. (9). (bottom) The temperature T_p of the probe when it is in both electrical equilibrium and thermal equilibrium with the nonequilibrium electron system in the graphene nanoribbon, calculated from Eq. (12).

were determined using the methods outlined in Ref. [30]. The linear-response coefficients were calculated using Eq. (4) following the methods of Refs. [19,20]. Additional details of our computational methods may be found in the Supplemental Material [31].

The top panel of Fig. 1 shows the Engquist-Anderson voltage $V_p^{\rm EA} \equiv -\mu_p^{\rm EA}/e$ computed from Eq. (8), while the bottom panel shows the thermoelectric correction ΔV_p to the probe voltage, computed from Eqs. (10)–(13). For this case, which is representative of various geometries we have considered (see Supplemental Material), the thermoelectric correction to the measured voltage is $\pm 24\%$ of the maximum voltage and $\pm 11.5\%$ of the applied bias, highlighting the importance of thermoelectric effects on precision voltage measurements in quantum systems. As mentioned previously, this system is not unique, and even larger corrections are expected for systems with larger thermoelectric responses.

The cause of the substantial thermoelectric correction to the voltage is elucidated in Fig. 2. The top panel of Fig. 2 shows the heat current $I_p^{(1)}$ flowing into the probe when its temperature is held constant at T_0, calculated using Eq. (9). The peak values of $I_p^{(1)} = \pm 2.3$ nW may not be large in an absolute sense, but they correspond to a heat current density of $j_p^{(1)} = 4.5 \times 10^{10}\,{\rm W/m^2}$ through the apex atom at the tip of the probe, some 700 times the radiant energy flux at the surface of the sun! Clearly, the assumption that such a probe, whose voltage is given by Eq. (8), is in local equilibrium with the system is questionable.

The bottom panel of Fig. 2 shows the deviation of the temperature T_p of an ideal thermoelectric probe from ambient temperature, calculated from Eq. (12). The ideal probe is in local thermal equilibrium with the system, and as such, its temperature maps out the hot and cold regions of the system

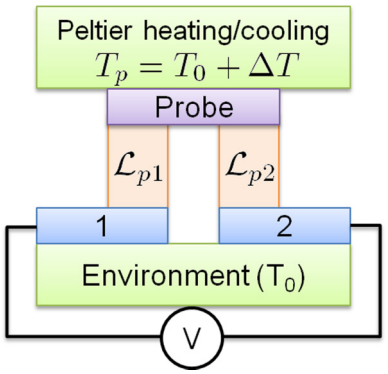

FIG. 3. (Color online) Thermoelectric circuit diagram for the three-terminal source-drain-probe circuit. According to Eqs. (9) and (12), there is Peltier heating (cooling) of the probe if $(\mathcal{L}^{(1)}_{p1}\mathcal{L}^{(0)}_{p2} - \mathcal{L}^{(1)}_{p2}\mathcal{L}^{(0)}_{p1})(\mu_1 - \mu_2) > 0$ (< 0). Equation (12) also includes a direct thermal coupling κ_{p0} of the probe to the environment (not shown in the diagram).

[19,20,32]. Hot and cold spots within the system arise due to local Peltier heating/cooling induced by the electrical bias between the source and drain electrodes, as described by Eqs. (9) and (12) and illustrated in Fig. 3. The three-terminal thermoelectric circuit formed by the source, drain, and probe electrodes is equivalent to that of a standard two-junction Peltier cooler/heater [33,34]. The difference is that in a macroscopic Peltier effect device, the materials forming the $p1$ and $p2$ junctions are distinct (typically, n type and p type) and physically separate, while in the present example both junctions are formed within the same quantum material. In the quantum transport regime, the $p1$ and $p2$ junctions will act like n-type and p-type channels, respectively, if the transmission functions from 1 to p and 2 to p are dominated by resonances below μ_0 and above μ_0, respectively. The bottom panel of Fig. 2 shows clear evidence of Peltier cooling/heating of up to ± 100 K within the system induced by an external electrical bias of 0.1 V. The large Peltier effect in this system may be related to giant thermoelectric effects predicted in related π-conjugated systems [26,27], where quantum interference effects have been shown to strongly enhance thermoelectricity. However, similar phenomena should occur in other ballistic quantum conductors.

Effect of thermal coupling of probe to environment

Let us now consider the effects of measurement nonideality. The greatest source of error in a scanning thermoelectric measurement is likely to stem from the unavoidable coupling κ_{p0} of the probe to the thermal background (typically, the ambient environment) [19]. Indeed, state-of-the-art SThM still operates in the regime where the coupling of the probe to the thermal background is many times its thermal coupling to the system itself [18]. While values of κ_{p0} much less than the thermal conductance quantum $\kappa_0 = (\pi^2/3)k_B^2 T_0/h$ (0.284 nW/K at 30 0K) [35] are possible in principle for probes whose thermal coupling to the environment is predominantly radiative [19], current scanning probes [18] have $\kappa_{p0} > 100\kappa_0$.

Figure 4 shows the thermoelectric correction to the voltage (top panel) and the probe temperature (bottom panel) for

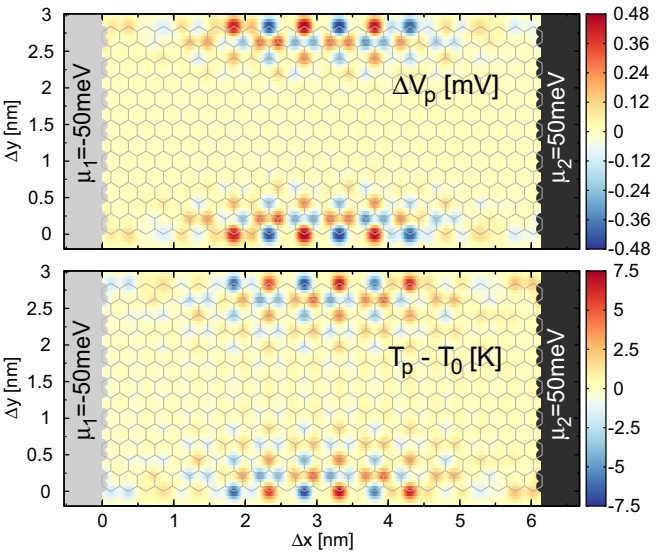

FIG. 4. (Color online) (top) The thermoelectric correction ΔV_p to the probe voltage and (bottom) the deviation of the probe temperature from ambient temperature for the same system as that shown in Figs. 1 and 2, but with a finite thermal coupling $\kappa_{p0} = \kappa_0$ of the probe to the environment, where $\kappa_0 = (\pi^2/3)k_B^2 T_0/h$ (0.284 nW/K at 300K) is the thermal conductance quantum. Equations (10) and (12) indicate that the thermoelectric corrections for larger values of κ_{p0} scale as κ_{p0}^{-1}.

$\kappa_{p0} = \kappa_0$. For this case, the thermal coupling of the probe to the environment exceeds its coupling to the system, so that the probe temperature is closer to ambient, and the thermoelectric correction to the voltage is reduced. The reduction of the thermoelectric corrections is described analytically by Eqs. (10) and (12). Even for a thermal coupling of $\kappa_{p0} = 700\kappa_0$, which is typical of current state-of-the-art SThM [18], the voltage error would still be of order 1 μV, well within the resolution of precision voltage measurements, which routinely obtain subangstrom spatial resolution [5].

V. CONCLUSIONS

An ideal voltage measurement in a nonequilibrium quantum system was defined in terms of a floating thermoelectric probe that reaches both electrical and thermal equilibrium with a system via local (e.g., tunnel) coupling. This definition extends Büttiker's quantum voltage probe paradigm [2,3] to systems at finite temperature, where thermoelectric effects are important. A previous work [13] which formally considered such an extension made the assumption that the scattering matrix is energy independent, so that thermoelectric effects are exponentially small, which is not the case in the present analysis.

As an example, we developed a realistic model of a scanning potentiometer with atomic resolution and used it to investigate voltage measurement in a prototypical ballistic quantum conductor (a graphene nanoribbon) bonded to source and drain electrodes. Under ideal measurement conditions, we predict large thermoelectric voltage corrections (~24% of the probe's peak voltage signal) when the applied source-drain bias voltage is small. We also derived expressions for

the probe's voltage correction under nonideal measurement conditions, finding that the voltage correction is reduced linearly as the probe-environment coupling is increased. In the graphene nanoribbon system considered here, voltage corrections on the order of several microvolts persist even with strong environmental coupling.

In summary, we predict a large thermoelectric correction to voltage measurement in quantum-coherent conductors. The origin of this correction is local Peltier cooling/heating within the nonequilibrium quantum system, a generic three-terminal thermoelectric effect. This finding has important implications for precision local electrical measurements: it implies that a precision voltage measurement requires a simultaneous precision temperature measurement.

ACKNOWLEDGMENTS

The authors wish to thank Markus Büttiker for useful discussions on the nature of voltage measurement in finite-temperature quantum systems. C.A.S. was supported by the U.S. Department of Energy, Office of Science, Award No. DE-SC0006699.

[1] H.-L. Engquist and P. W. Anderson, Phys. Rev. B **24**, 1151 (1981).
[2] M. Büttiker, IBM J. Res. Dev. **32**, 63 (1988).
[3] M. Büttiker, Phys. Rev. B **40**, 3409 (1989).
[4] H. Förster, P. Samuelsson, S. Pilgram, and M. Büttiker, Phys. Rev. B **75**, 035340 (2007).
[5] S. V. Kalinin and A. Gruverman, *Scanning Probe Microscopy: Electrical and Electromechanical Phenomena at the Nanoscale* (Springer, New York, 2007), Vol. 1.
[6] A. D. Benoit, S. Washburn, C. P. Umbach, R. B. Laibowitz, and R. A. Webb, Phys. Rev. Lett. **57**, 1765 (1986).
[7] K. L. Shepard, M. L. Roukes, and B. P. van der Gaag, Phys. Rev. B **46**, 9648 (1992).
[8] R. de Picciotto, H. Stormer, L. Pfeiffer, K. Baldwin, and K. West, Nature (London) **411**, 51 (2001).
[9] B. Gao, Y. F. Chen, M. S. Fuhrer, D. C. Glattli, and A. Bachtold, Phys. Rev. Lett. **95**, 196802 (2005).
[10] M. Bolsterli, M. Rich, and W. M. Visscher, Phys. Rev. A **1**, 1086 (1970).
[11] K. Sääskilahti, J. Oksanen, and J. Tulkki, Phys. Rev. E **88**, 012128 (2013).
[12] D. Roy and A. Dhar, Phys. Rev. B **75**, 195110 (2007).
[13] P. A. Jacquet, J. Stat. Phys. **134**, 709 (2009).
[14] D. Sánchez and L. Serra, Phys. Rev. B **84**, 201307 (2011).
[15] A. Caso, L. Arrachea, and G. S. Lozano, Phys. Rev. B **83**, 165419 (2011).
[16] P. A. Jacquet and C.-A. Pillet, Phys. Rev. B **85**, 125120 (2012).
[17] A. Majumdar, Annu. Rev. Mater. Sci. **29**, 505 (1999).
[18] K. Kim, W. Jeong, W. Lee, and P. Reddy, ACS Nano **6**, 4248 (2012).
[19] J. P. Bergfield, S. M. Story, R. C. Stafford, and C. A. Stafford, ACS Nano **7**, 4429 (2013).
[20] J. P. Bergfield, M. A. Ratner, C. A. Stafford, and M. Di Ventra, arXiv:1305.6602 .
[21] K. Kim, J. Chung, G. Hwang, O. Kwon, and J. S. Lee, ACS Nano **5**, 8700 (2011).
[22] Y.-J. Yu, M. Y. Han, S. Berciaud, A. B. Georgescu, T. F. Heinz, L. E. Brus, K. S. Kim, and P. Kim, Appl. Phys. Lett. **99**, 183105 (2011).
[23] F. Menges, H. Riel, A. Stemmer, and B. Gotsmann, Nano Lett. **12**, 596 (2012).
[24] L. Onsager, Phys. Rev. **37**, 405 (1931).
[25] U. Sivan and Y. Imry, Phys. Rev. B **33**, 551 (1986).
[26] J. P. Bergfield and C. A. Stafford, Nano Lett. **9**, 3072 (2009).
[27] J. P. Bergfield, M. A. Solis, and C. A. Stafford, ACS Nano **4**, 5314 (2010).
[28] S. Datta, *Electronic Transport in Mesoscopic Systems* (Cambridge University Press, Cambridge, 1995).
[29] S. Reich, J. Maultzsch, C. Thomsen, and P. Ordejon, Phys. Rev. B **66**, 035412 (2002).
[30] C. J. Chen, *Introduction to Scanning Tunneling Microscopy*, 2nd ed. (Oxford University Press, New York, 1993).
[31] See Supplemental Material at http://link.aps.org/supplemental/10.1103/PhysRevB.90.235438 for a discussion of the thermoelectric correction for strong probe-environment coupling and a detailed description of our computational methods.
[32] J. Meair, J. P. Bergfield, C. A. Stafford, and P. Jacquod, Phys. Rev. B **90**, 035407 (2014).
[33] F. J. DiSalvo, Science **285**, 703 (1999).
[34] L. E. Bell, Science **321**, 1457 (2008).
[35] L. G. C. Rego and G. Kirczenow, Phys. Rev. Lett. **81**, 232 (1998).